4. WHOLE ROCK GEOCHEMISTRY

4.1. Introduction

Sixty samples from all major rock units have been analysed for major and selected trace elements by XRF at the University of Pretoria, using an ARL 8420 wavelength dispersive spectrometer. Analytical procedures are given in Appendix I and the analyses are listed in Appendix II. Thirty-six samples were analysed for additional trace elements, including REE, by ICP-MS at the University of Cape Town. Sulphur was separately determined for all samples by LECO – titration at the University of Quebec at Chicoutimi. Copper was determined by atomic absorption and the PGE were determined by INAA, all at the University of Quebec at Chicoutimi. This chapter presents the major and trace element data to ascertain effects of alteration, the crystallisation trends with the aid of variation diagrams and the overall mineral distribution throughout the Complex.

4.2. The Effects of Alteration on Major-, Trace- and Rare Earth Element Concentration

It has been pointed out in the previous chapter that many of the rocks of the Uitkomst Complex are highly altered. The alteration may overprint the original geochemical signatures of the rocks and thereby render the determination of the genesis of the Complex and its mineralization difficult. It is therefore important to determine which of the analysed elements behaved in a mobile manner during alteration.

Zirconium has been shown to be relatively immobile during alteration and high-grade metamorphism, for example in the Sao Francisco craton of Brazil (Figueiredo, 1980). Thus, incompatible elements that have remained immobile during alteration should correlate closely with Zr. Most of the REE have apparently remained immobile (e.g. La, Yb, Lu) as is evidenced by their good positive correlation with Zr (Fig. 4.1. (a)). Elements that show a poor correlation with Zr, for example Rb, Th (Fig. 4.1. (b)), P, Ti, K (Fig. 4.2.) and, to a lesser extent, Na (not shown) and Eu (Fig. 4.1. (a)) may have been affected by

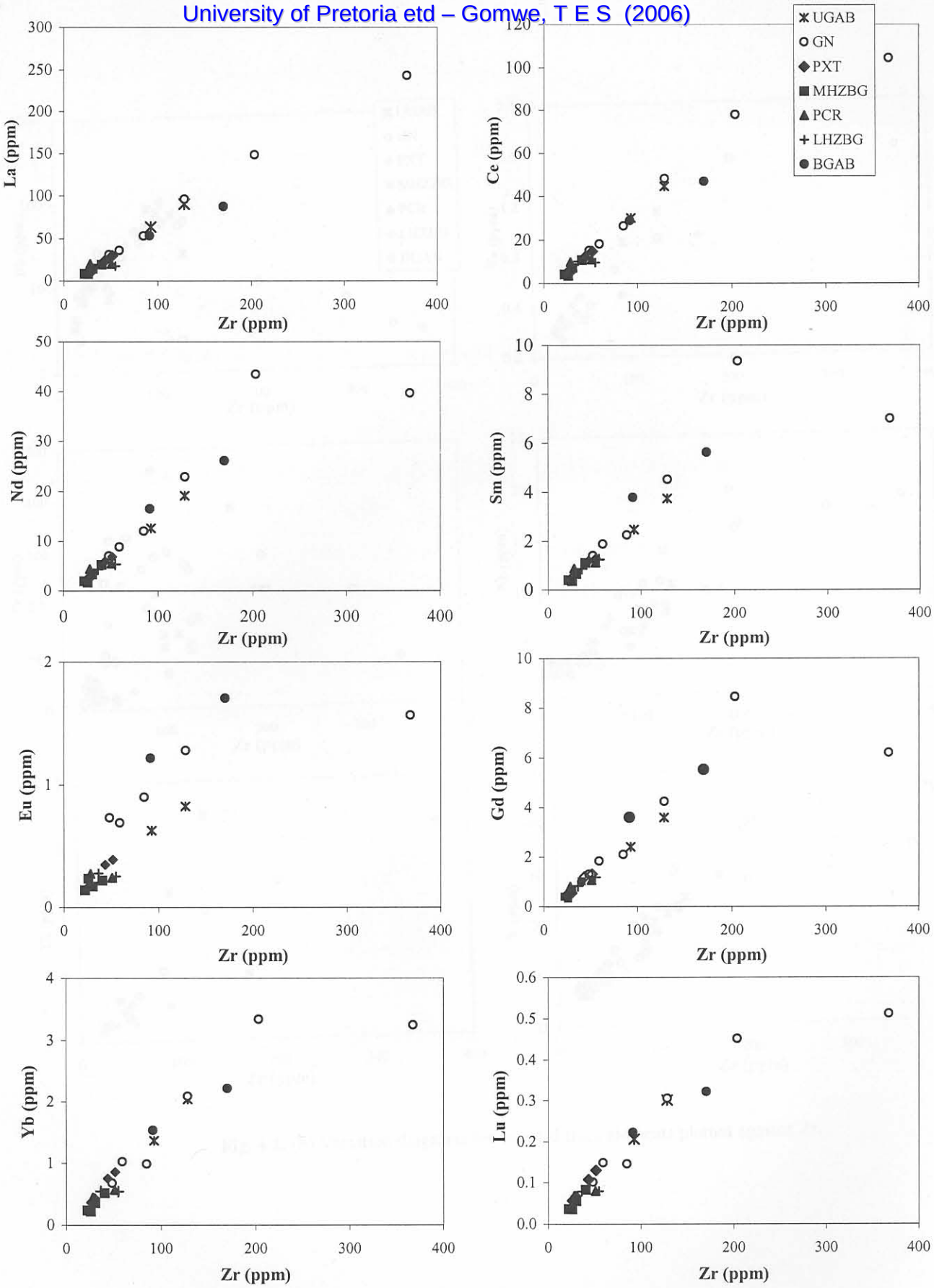

Fig. 4.1. (a) Variation diagrams of selected REE versus Zr

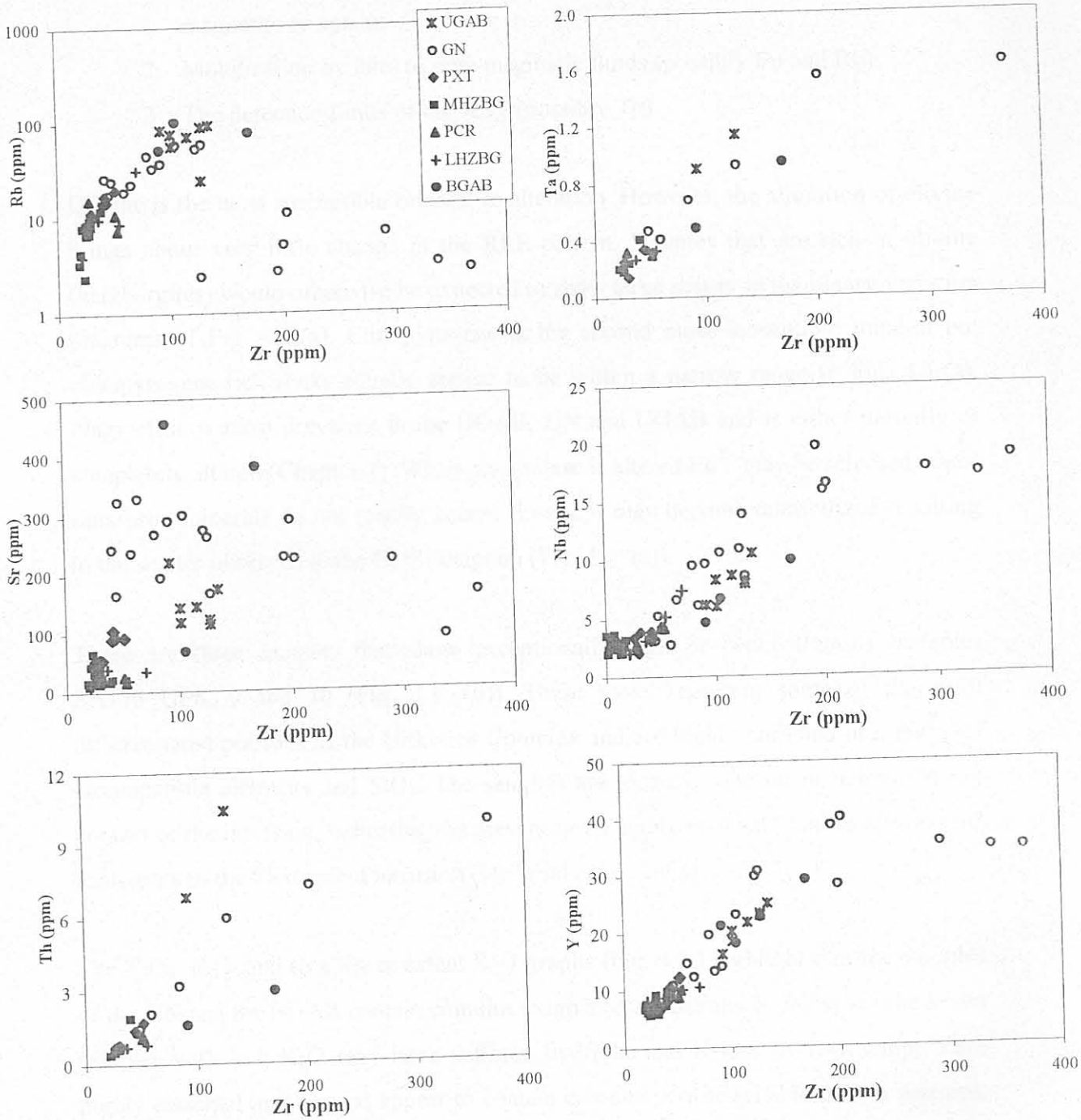

Fig. 4.1. (b) Variation diagrams for selected trace elements plotted against Zr.

1. The intermittent appearance or disappearance of a cumulus phase e.g. magnetite or apatite.
2. Mobilization by late- to post-magmatic fluids (possibly Eu and Rb).
3. The detection limits of the XRF (possibly Th).

Olivine is the most susceptible mineral to alteration. However, the alteration of olivine brings about very little change in the REE pattern. Samples that are rich in olivine (harzburgites) would otherwise be expected to show large scatter in the binary variation diagrams of Fig. 4.1.(a). Clinopyroxene is the second most susceptible mineral but clinopyroxene-rich rocks equally appear to be within a narrow range in Fig. 4.1.(a). Plagioclase is most prevalent in the BGAB, GN and UGAB and is either partially or completely altered (Chapter 3). When plagioclase is altered Eu^{2+} may be released, since saussurite minerals do not readily accept Eu and it may become remobilized resulting in the scatter observed in the Eu/Zr diagram (Fig. 4.1. (a)).

There are three samples that show exceptionally high Zr concentrations (samples SH176 UP8, 9 and 10 (Fig. 4.1. (b)). These rocks represent some of the most differentiated portions of the Uitkomst Complex and are highly enriched in a range of incompatible elements and SiO_2. The samples are located some 60 m below the top contact of the intrusion, indicating the presence of a highly evolved "sandwich horizon" analogous to the Skaergaard intrusion (De Waal *et al.*, 2001).

The TiO_2, P_2O_5 and to a lesser extent K_2O graphs (Fig. 4.2.) highlight that the samples of the GN and the BGAB contain cumulus magnetite, apatite and K-feldspar. The seven samples with low K_2O may have suffered hydrothermal K-loss. A few samples are highly enriched in P_2O_5 and appear to contain cumulus apatite (visible in thin sections, Chapter 3). Notably, they are not particularly SiO_2 or Zr-enriched, indicating that cumulus apatite appeared before zircon.

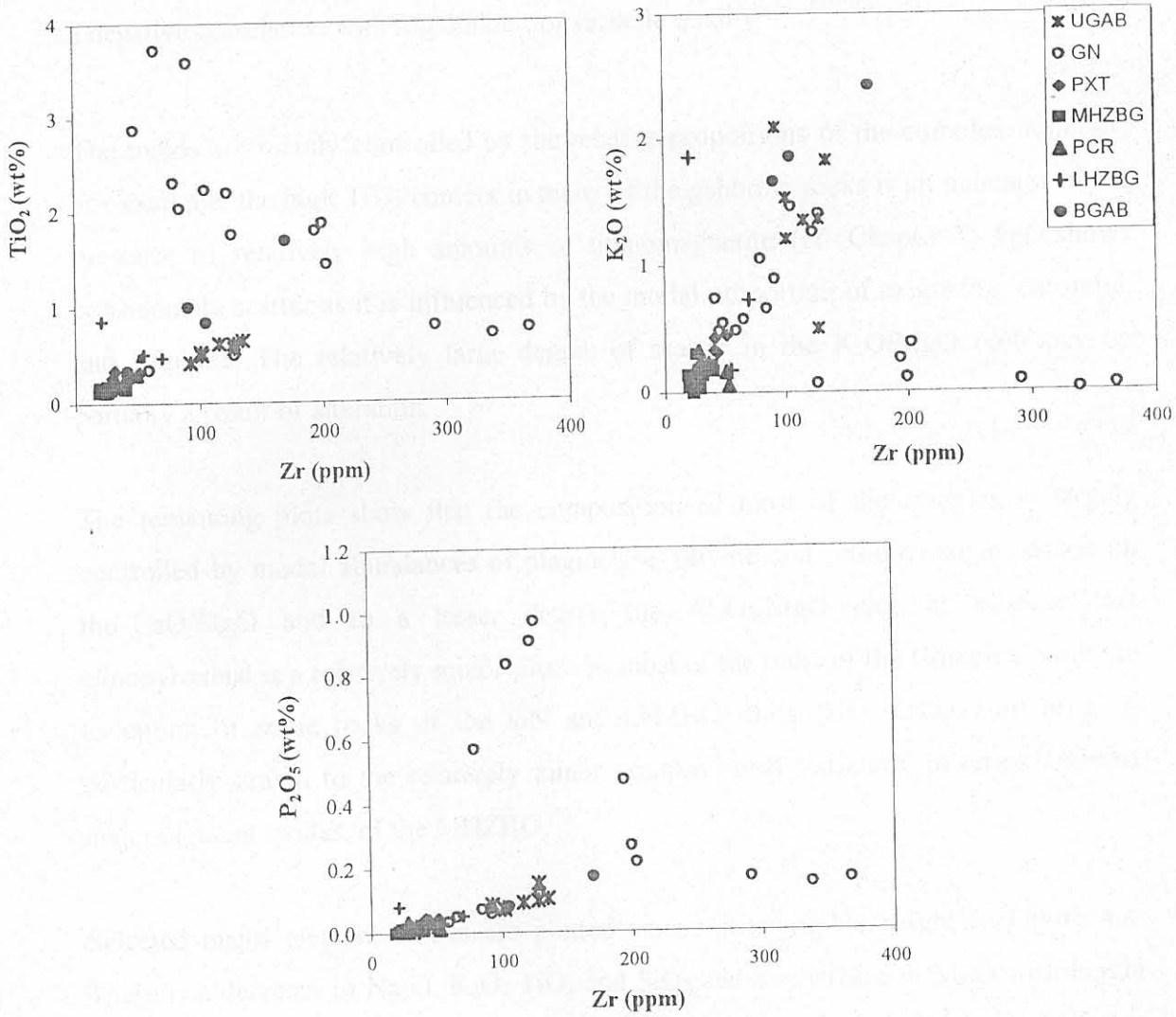

Fig.4.2. Variation diagrams for selected element oxides plotted against Zr

4.3. Major Element Chemistry

In general, more primitive igneous rocks are richer in MgO and poorer in FeO, Na_2O, K_2O, CaO and SiO_2 than more evolved rocks. Thus these oxides alone or in some combination, may be used as indices of differentiation. Selected major element oxides are plotted against MgO in Figure 4.3. Apart from FeO, all major element oxides show a negative correlation with MgO albeit of variable quality.

The trends are mainly controlled by the relative proportions of the cumulus minerals. For example, the high TiO_2 content in many of the gabbroic rocks is an indicator of the presence of relatively high amounts of titanomagnetite (cf. Chapter 3). FeO shows considerable scatter as it is influenced by the modal proportion of magnetite, chromite, and sulphide. The relatively large degree of scatter in the K_2O/MgO plot may be partially a result of alteration.

The remaining plots show that the composition of most of the samples is largely controlled by modal abundances of plagioclase, olivine and orthopyroxene. Based on the CaO/MgO and, to a lesser degree, the Al_2O_3/MgO plot, it is clear that clinopyroxene is a relatively minor phase in most of the units of the Complex, with the exception of some rocks of the GN and LHZBG units. The reader's attention is particularly drawn to the relatively minor compositional variation, in terms of most major element oxides, of the MHZBG.

Selected major element oxides are plotted versus stratigraphic height in Figure 4.4. There is a decrease in Na_2O, K_2O, TiO_2 and SiO_2 and an increase in MgO with height from the base of the Complex to the base of the MHZBG which is opposite of what is expected in a progressively differentiating magma chamber. The most noticeable feature of the diagrams is the primitive nature of the MHZBG indicated by the relatively low Na_2O, K_2O, TiO_2 and SiO_2 and high MgO values and the lack of variation of these oxides with height. The latter feature is again contrary to the trend expected during differentiation upon cooling. From the top of the MHZBG to the top of the GN, normal differentiation trends are observed, but a marked reversal is seen at the base of the UGAB.

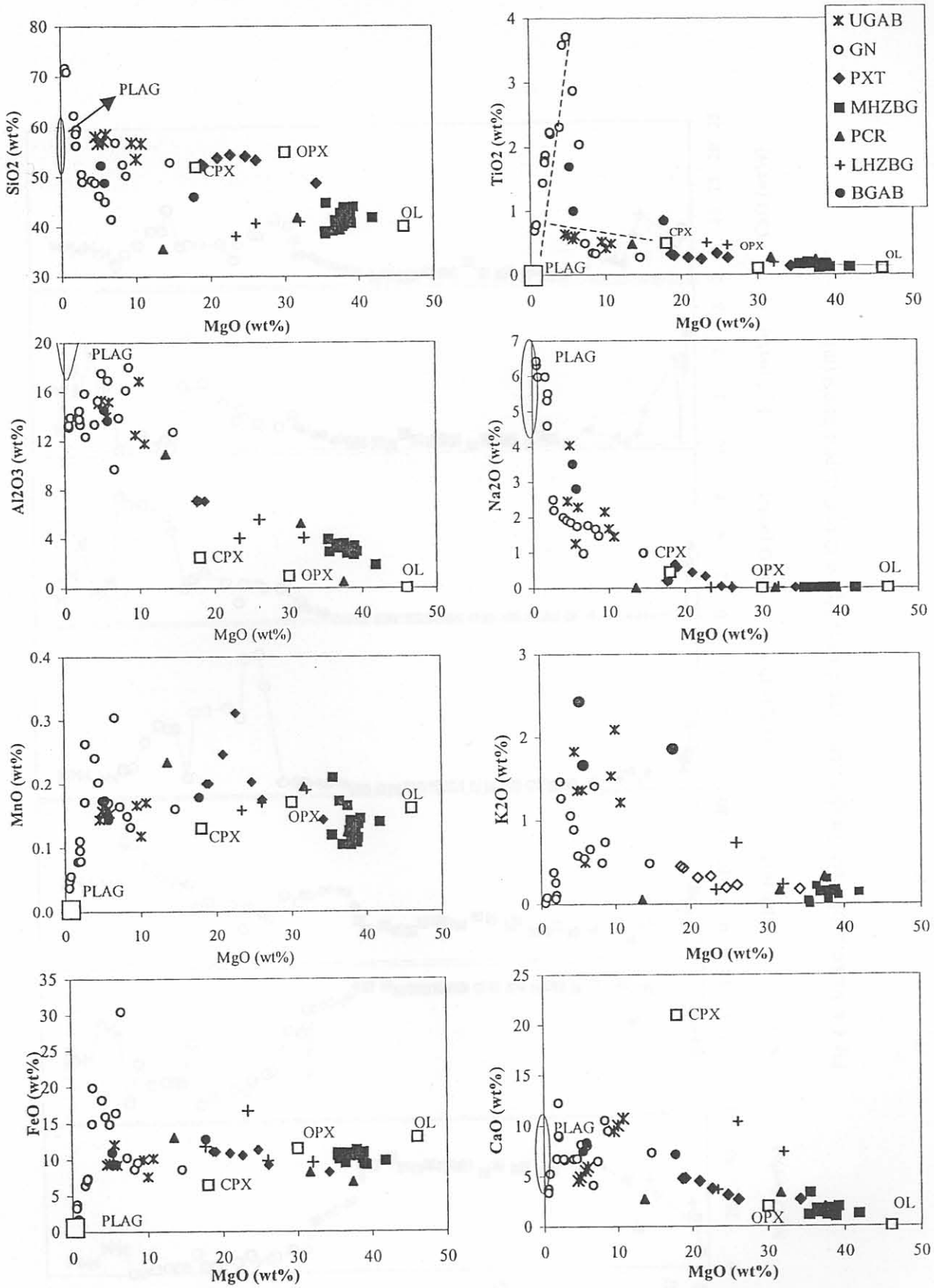

Fig. 4.3. Variation diagrams for major elements, plotted against MgO.
(Compositions of mineral phases are from Gauert (1998))

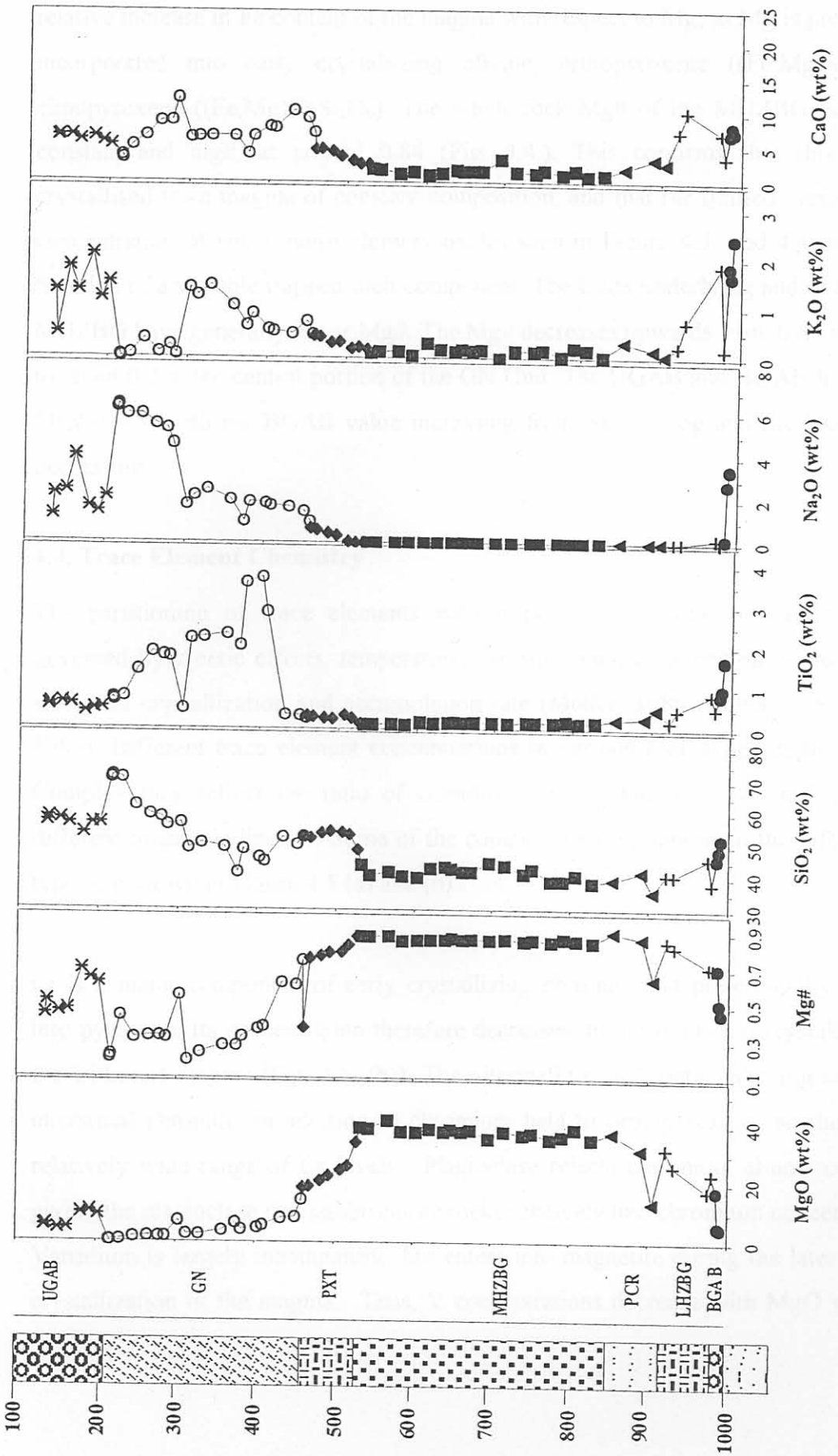

Fig.4.4. Variation of selected major element oxides and Mg# with stratigraphic height (m).

The variation of the Mg number (calculated as the ratio MgO/(MgO + FeO) and hereafter abbreviated to Mg#) reflects the fractionation trend of magma, namely the relative increase in Fe content of the magma with respect to Mg, as Mg is preferentially incorporated into early crystallizing olivine, orthopyroxene ($(Fe,Mg)Si_2O_6$) and clinopyroxene ($(Fe,Mg)CaSi_2O_6$). The whole-rock Mg# of the MHZBG is relatively constant and high, at around 0.84 (Fig. 4.4.). This confirms that this Unit has crystallised from magma of constant composition, and that the limited variation in the concentration of some major element oxides seen in Figure 4.3. and 4.4. is largely a function of a variable trapped melt component. The Units underlying and overlying the MHZBG have generally lower Mg#. The Mg# decreases upwards from 0.84 in the PXT to about 0.2 in the central portion of the GN Unit. The UGAB and BGAB have similar Mg# (~0.5) with the BGAB value increasing from base to top and the UGAB value decreasing.

4.4. Trace Element Chemistry

The partitioning of trace elements with respect to the rock-forming minerals is governed by kinetic effects, temperature, pressure, melt composition, ionic radii, site sizes and crystallization and accumulation rate (Möller, 1988; Ulmer, 1989; Hanson, 1989). Different trace element concentrations in various rock types of the Uitkomst Complex may reflect the ratio of cumulus to intercumulus phases and possibly a different magmatic lineage. Some of the compositional variations in the different rock types are shown in Figure 4.5.(a) and (b).

Cr is a major component of early crystallizing chromite and preferentially partitions into pyroxene. Its concentration therefore decreases during fractional crystallization of the Uitkomst magma (Fig. 4.5. (b)). The ultramafic rocks contain varying amounts of interstitial chromite, in addition to chromium held in orthopyroxene, so they show a relatively wide range of Cr levels. Plagioclase rejects chromium almost completely giving the plagioclase rich gabbronorite rocks relatively low chromium concentrations. Vanadium is largely incompatible, but enters into magnetite during the later stages of crystallization of the magma. Thus, V concentrations decrease with MgO within the

GN (Fig. 4.5. (a)). The exceptionally high V value in one sample from the GN is attributed to the abundance of titanomagnetite, which can be identified in thin section.

Strontium has an ionic radius of 1.18Å allowing it to substitute for Ca (1.01Å) (D = 1.83, Rollinson, 1993) and K (1.33Å). The partitioning of Sr into plagioclase is more pronounced than into other cumulus phases and ultramafic rocks show depletion in Sr relative to norites and gabbronorites of the BGAB and GN units (Fig. 4.5.(a)). There is a variation factor of about 5 in the gabbroic Units amongst samples with the same MgO content (about 5%) indicating the presence of Mg-free phases other than plagioclase, including quartz, magnetite, and K-feldspar, which all accommodate little or no Sr.

P_2O_5 is present only in trace to minor amounts and behaves as an incompatible element throughout much of the Complex. However, in some of the GN samples P_2O_5 contents increase significantly, due to the crystallization of apatite (Chapter 3).

Rb, Y, Nb, Th, Ta, P and Zr and the REE (D values less than unity) do not enter significantly into other cation sites in the major cumulus minerals of the Uitkomst Complex apart from Rb into K-feldspar (D = 3.06, Rollinson, 1993) in the GN. These elements become concentrated in the magma during differentiation until minerals such as zircon and apatite crystallize at a late stage. Low concentrations of Zr, Y and Rb in the ultramafic rocks therefore indicate the primitive nature of the magma and low proportions of trapped melt. Assuming that the Uitkomst Complex crystallized from magma similar to the B1-type magma of the Bushveld Complex (De Waal *et al.*, 2001), the ultramafic rocks contain about 20-30% trapped melt. This is in accord with the petrographic determinations, indicating roughly 20% intercumulus material. The gabbroic rocks show the largest variation in highly incompatible trace elements (Fig. 4.5. (a) and (b)) indicative of their enrichment in the differentiating magma. The gabbroic rocks should show the appearance of K-feldspar, apatite, zircon, and possibly trace amounts of other phases such as monazite, sphene etc. however these could not be petrographically identified, due to the pervasive alteration of the differentiated rocks of the Complex.

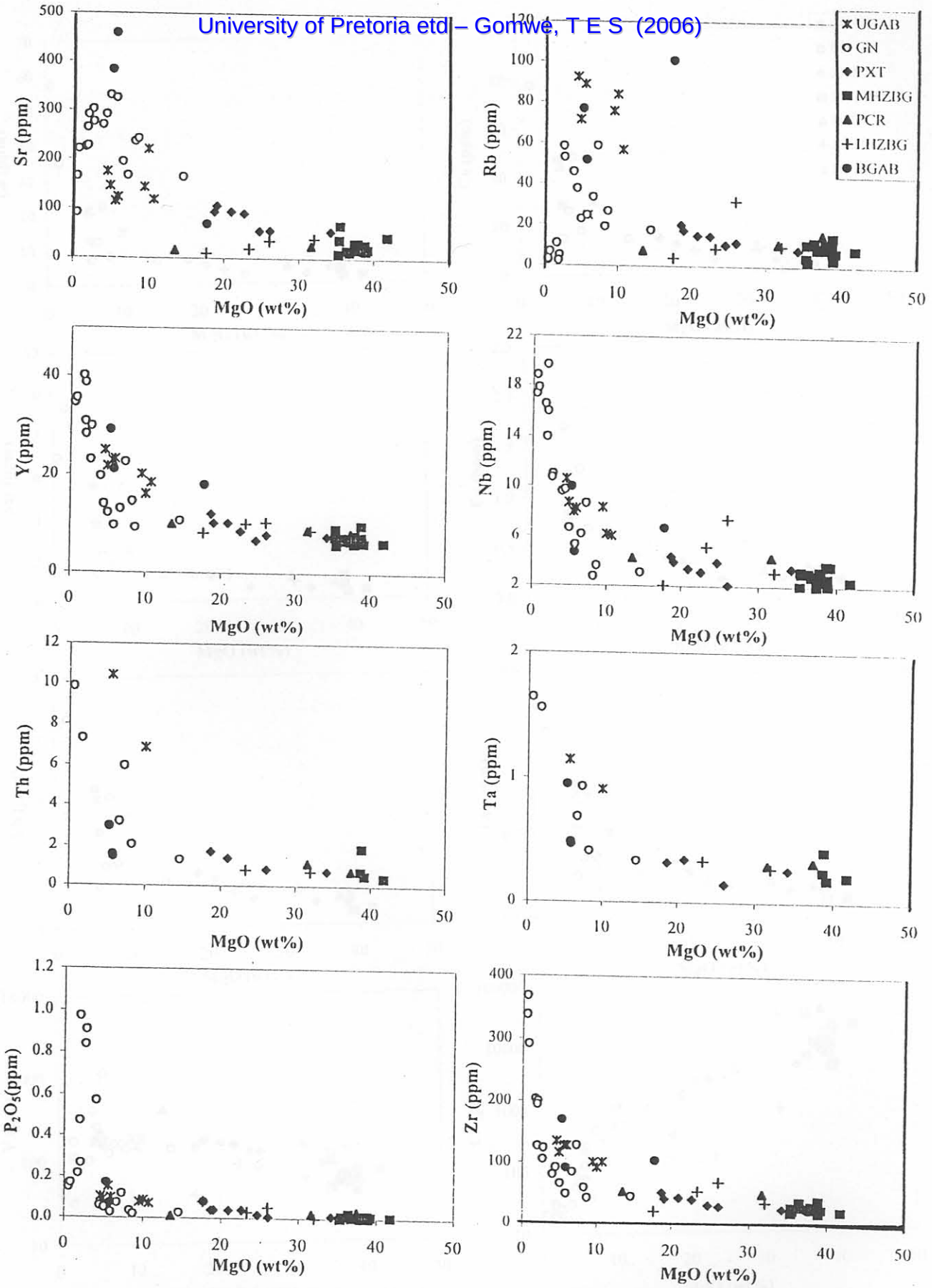

Fig.4.5.(a) Variation diagrams for selected trace elements versus MgO.

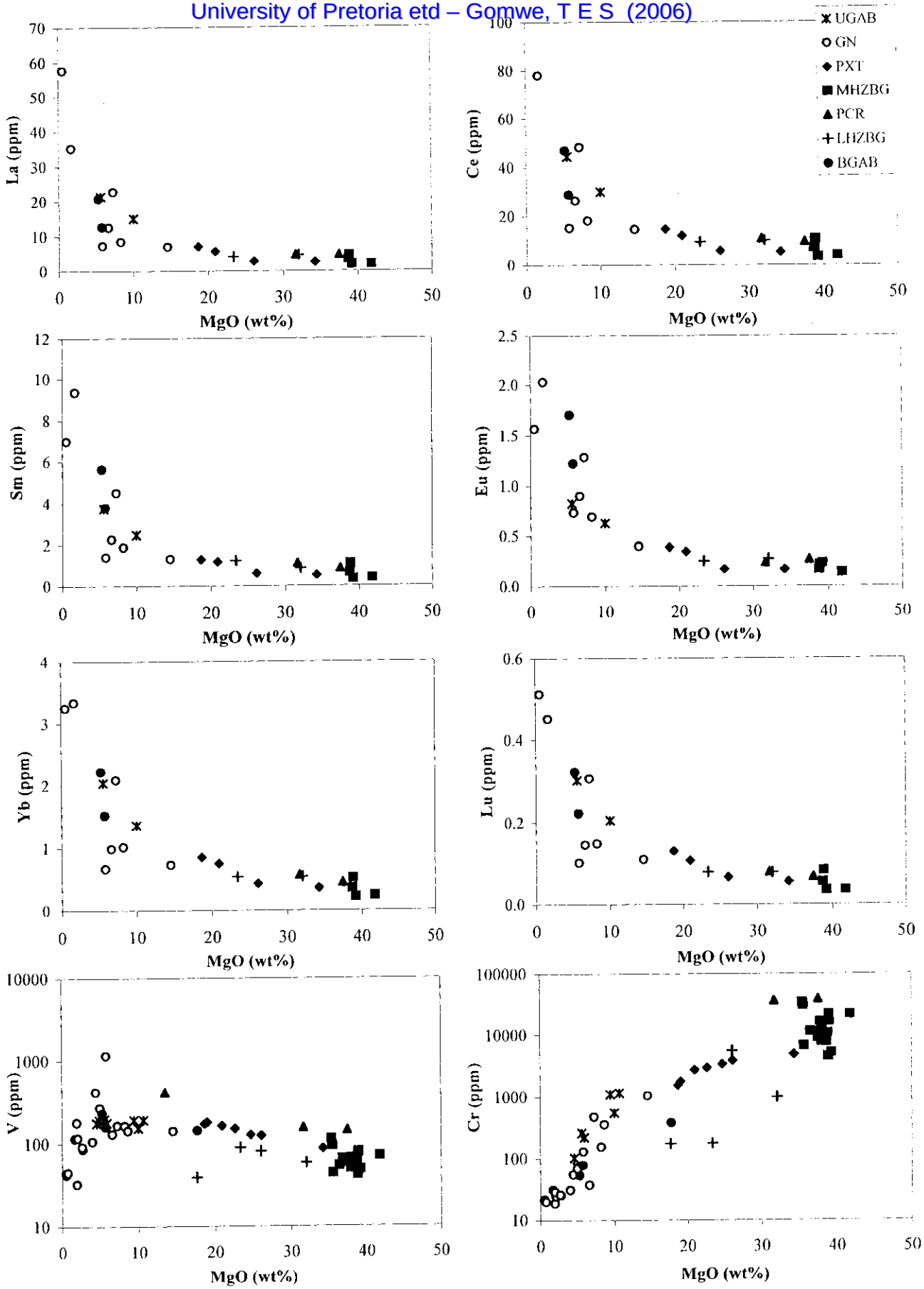

Fig.4.5.(b) Variation diagrams for selected trace elements and REE versus MgO.

Copper partitions preferentially into sulphides (Barnes and Maier, 1999) and Cu contents above 10-20 ppm indicate the presence of excess sulphide relative to the trapped melt. Fig. 4.6. shows that most of the samples have Cu values greater than this and that there is no direct correlation between Cu and MgO concentration, indicating the presence of cumulus sulphide. This point is also stressed by the plot of C/Zr versus MgO (Fig. 4.6.). The Cu/Zr ratio in the parental magma of the Bushveld Complex (B1) and of the chilled margins of the Uitkomst Complex is about 1. Therefore, if the Complex were a closed system, the bulk value of the Uitkomst Complex should equally be one. However, most of the Units show values exceeding unity (Fig. 4.6.), showing that most rocks of the Uitkomst Complex contain cumulus sulphides. In the UGAB and GN, Cu/Zr is <1, indicating that these rocks crystallized from metal depleted magma that had experienced a previous sulphide segregation event.

Nickel shows a relatively good positive correlation with MgO, particularly in the GN and UGAB Units. This is due to the compatible behaviour of Ni with respect to olivine (D=5.9-2.9), pyroxenes and chromite (D=29). In the BGAB and the ultramafic units the presence of sulphides overprints the signature of the silicates and chromite.

Cobalt also partitions into sulphides (D = 70, Barnes and Maier, 1999) as well as spinel (D=7.4 for magnetite, Rollinson, 1993) and olivine (D=6.6, Rollinson, 1993). Thus, in the sulphide-poor lithologies cobalt concentrations depend largely on modal proportions of olivine and chromite. This is reflected by the relatively high Co content of the sulphide-poor MHZBG Unit (Fig. 4.6.). In contrast, many samples from the sulphide-poor gabbroic rocks have low Co concentrations.

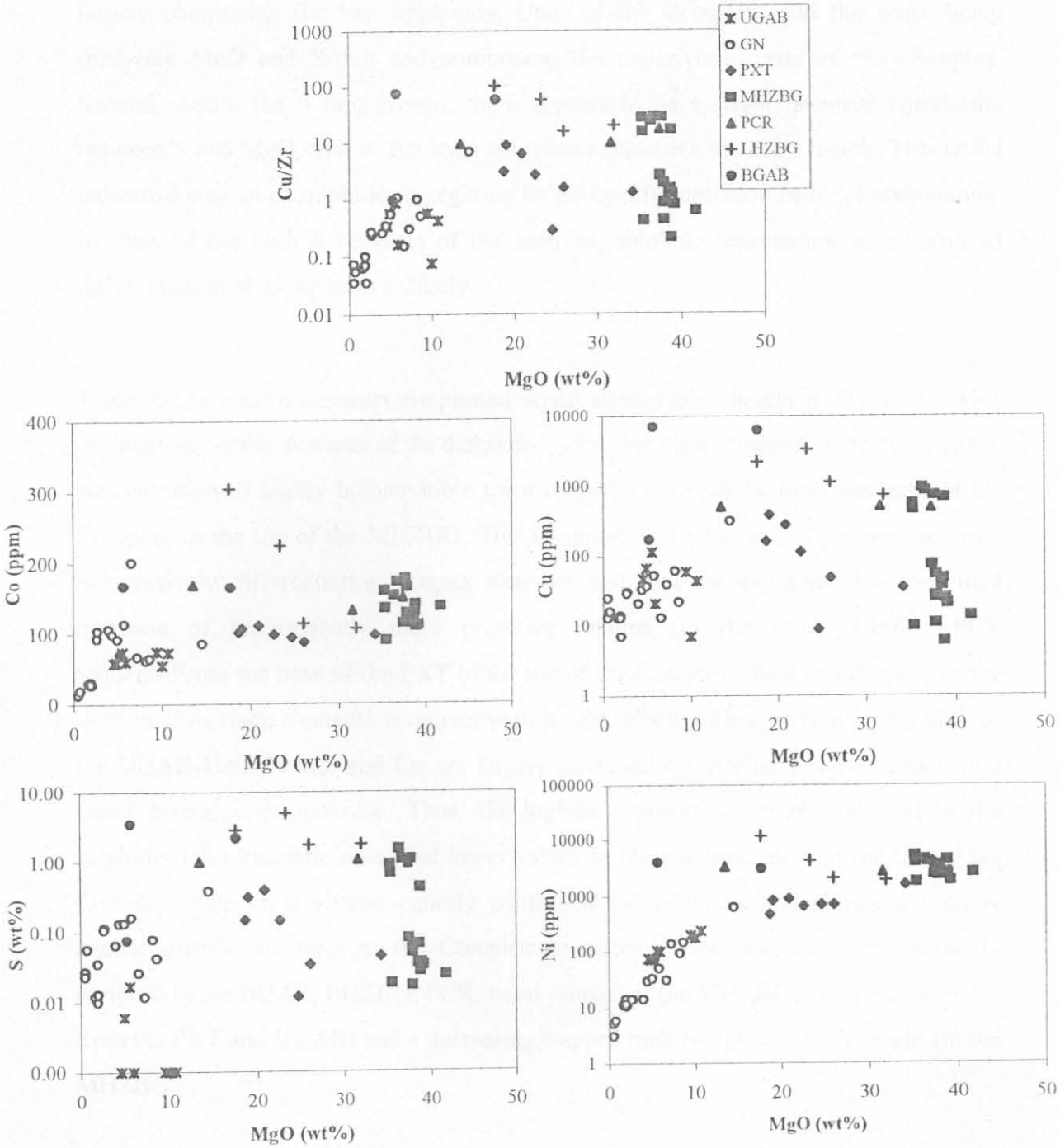

Fig.4.6. Variation diagrams for Cu/Zr and selected chalcophile trace elements plotted against MgO.

Several features are noteworthy in the S/MgO plot (Fig. 4.6.). First, the samples appear to fall into two distinct compositional fields, one being relatively MgO and S-poor and largely comprising the two uppermost Units of the Complex, and the other being relatively MgO and S-rich and comprising the underlying Units of the Complex. Second, within the S rich groups, there appears to be a slight negative correlation between S and MgO, that is, the least magnesian rocks are the most S-rich. This could indicate a control of sulphide segregation by either differentiation or by contamination. In view of the high S contents of the samples, sulphide segregation as a result of differentiation alone appears unlikely.

Trace and rare earth elements are plotted versus stratigraphic height in Figure 4.7. One of the most notable features of the diagrams is that there is a progressive decrease in the concentration of highly incompatible trace elements with height from the base of the Complex to the top of the MHZBG. This is opposite to what would be expected in a progressively differentiating magma chamber and may be explained by combined intrusion of progressively more primitive magma (in the BGAB-LHZBG-PCR sequenceFrom the base of the PXT to the top of the Complex, the concentration of the incompatible trace elements increases with height, albeit with a reverse at the base of the UGAB Unit. Nickel and Co are largely governed by sulphides, olivine and, to a lesser extent, orthopyroxene. Thus, the highest concentrations are observed in the sulphide-rich ultramafic units and lower values in the gabbroic units at the top of the Complex. Copper is almost entirely controlled by sulphides and shows a broadly similar distribution through the Complex as sulphur. Both elements are markedly enriched in the BGAB, LHZBG, PCR, basal portion of the MHZBG, and some samples from the PXT and UGAB) and a decreasing trapped melt component with height (in the MHZBG).

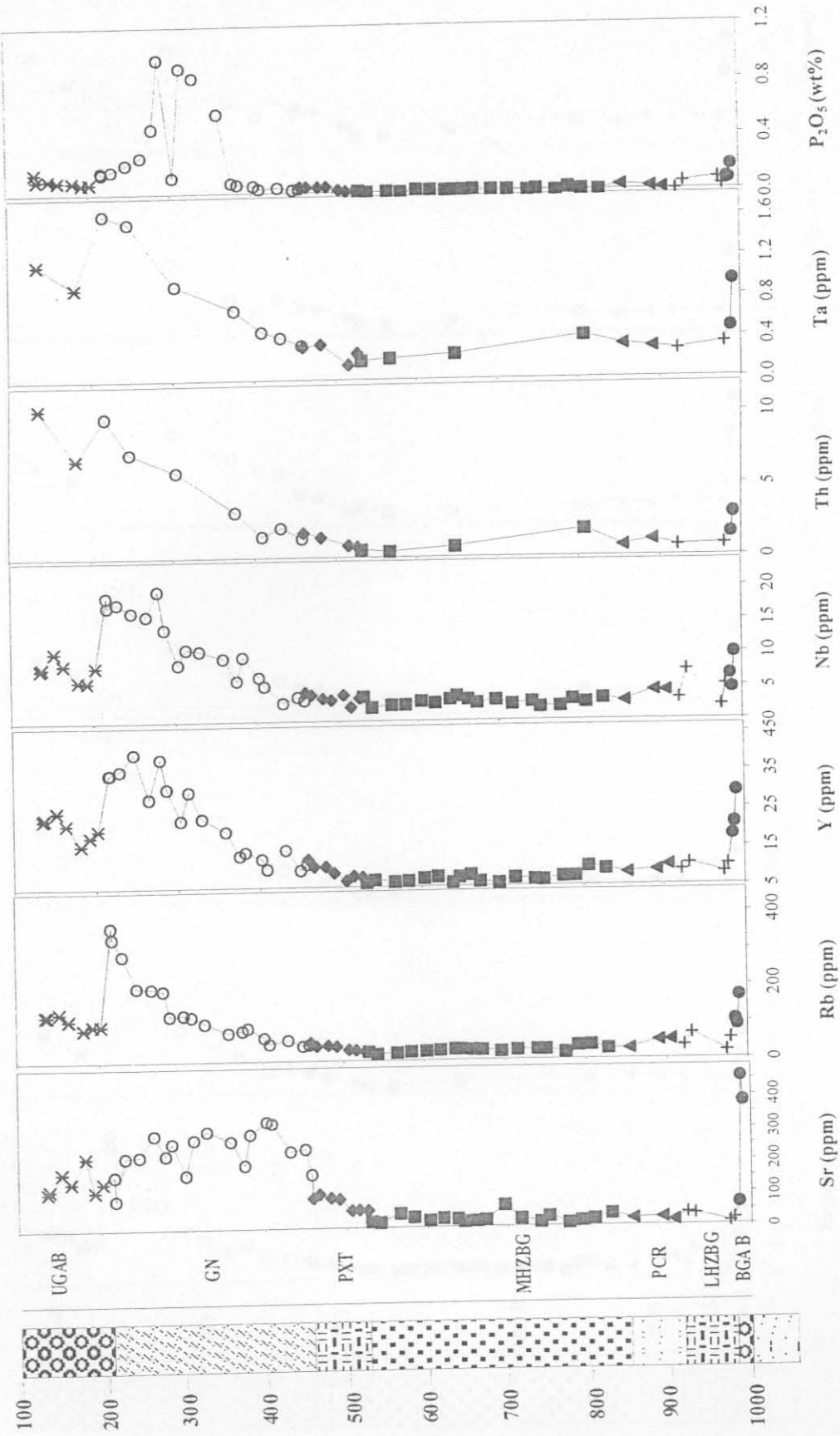

Fig.4.7. (a) Variation diagrams for selected trace elements versus stratigraphic height (m).

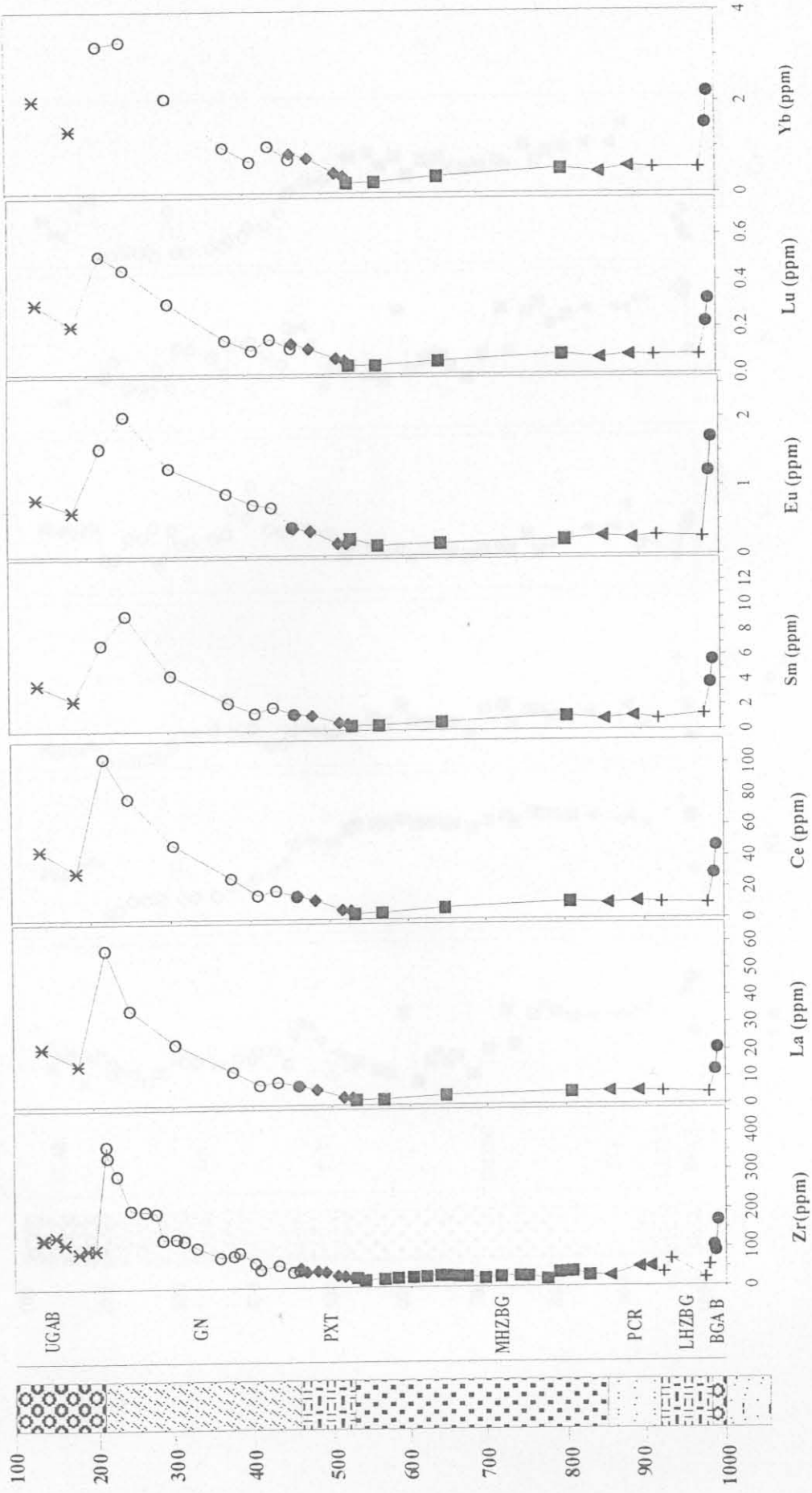

Fig.4.7. (b) Variation diagrams for selected trace elements versus stratigraphic height (m).

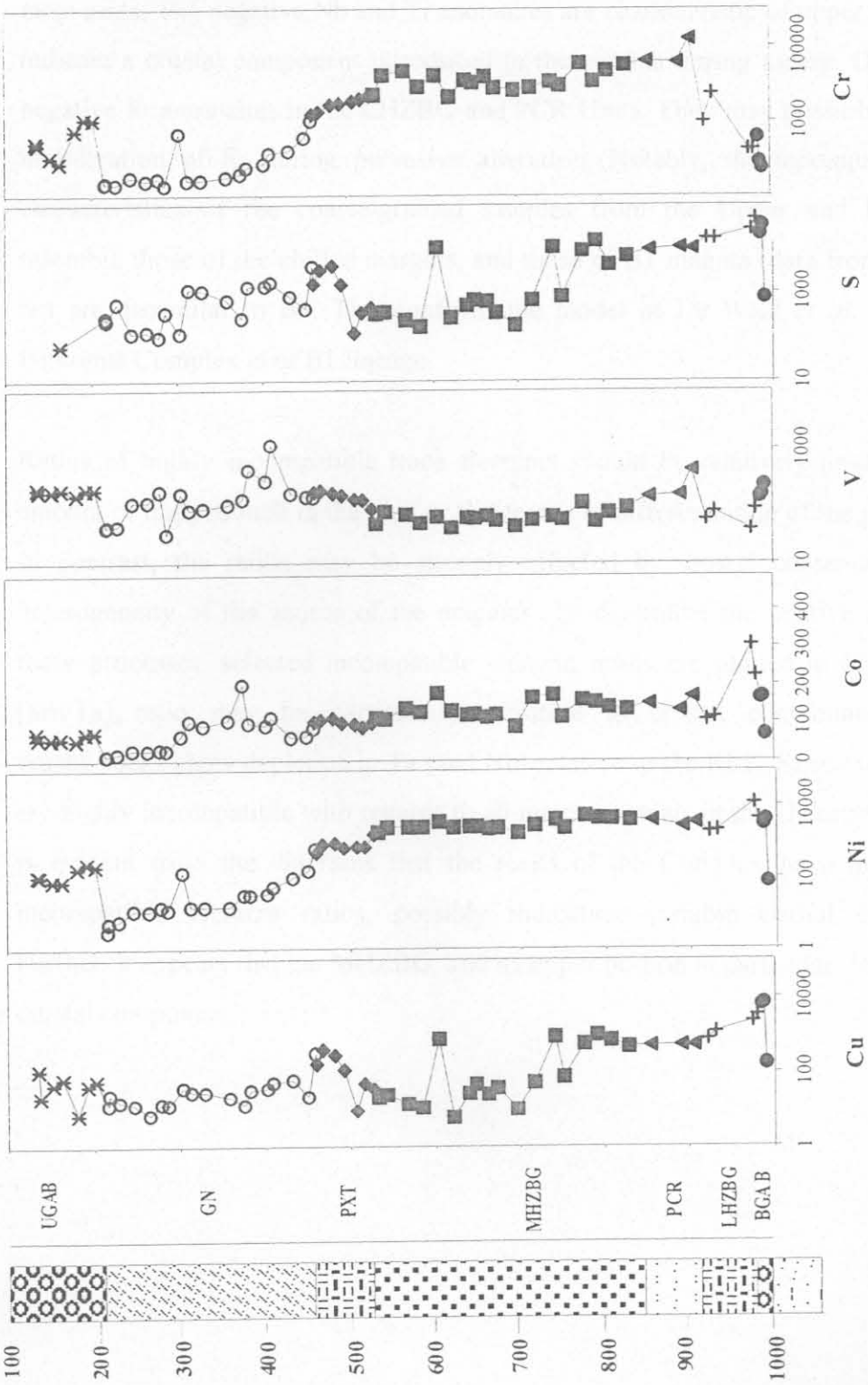

Fig.4.7(c) Variation diagrams for selected trace elements (ppm) versus stratigraphic height (m).

Spider diagrams of incompatible trace elements show that there is a similarity in shape between the units of the Complex (Fig. 4.8.). There is a negative Ti and Nb anomaly in most units. The negative Nb and Ti anomalies are characteristic of upper crust and may indicate a crustal component introduced to the magma during ascent. Of note are the negative Sr anomalies in the LHZBG and PCR Units. They may possibly be related to mobilization of Sr during pervasive alteration. Notably, the incompatible element characteristics of the coarse-grained samples from the Upper and Basal Gabbro resemble those of the chilled margins, and those of B1 magma (data from Curl, 2001), but are dissimilar to B3. This confirms the model of De Waal *et al.* 2001 that the Uitkomst Complex is of B1 lineage.

Ratios of highly incompatible trace elements should be relatively unaffected by the amount of trapped melt in the rock or the degree of differentiation of the parent magma. In contrast, the ratios may be strongly affected by crustal contamination, or by heterogeneity of the source of the magmas. To determine the relative importance of these processes, selected incompatible element ratios are plotted in Figure 4.9. The $[Sm/Ta]_n$ ratio may be particularly sensitive to crustal contamination, as many crustal rocks show depletion in Ta (and Nb) relative to the REE. Samarium, Th and Ta are highly incompatible with regards to all major minerals in the Uitkomst Complex. It is evident from the diagrams that the rocks of the Complex have highly variable incompatible element ratios, possibly indicating variable crustal contamination. Further, it appears that the MHZBG, and its upper portion in particular, have the lowest crustal component.

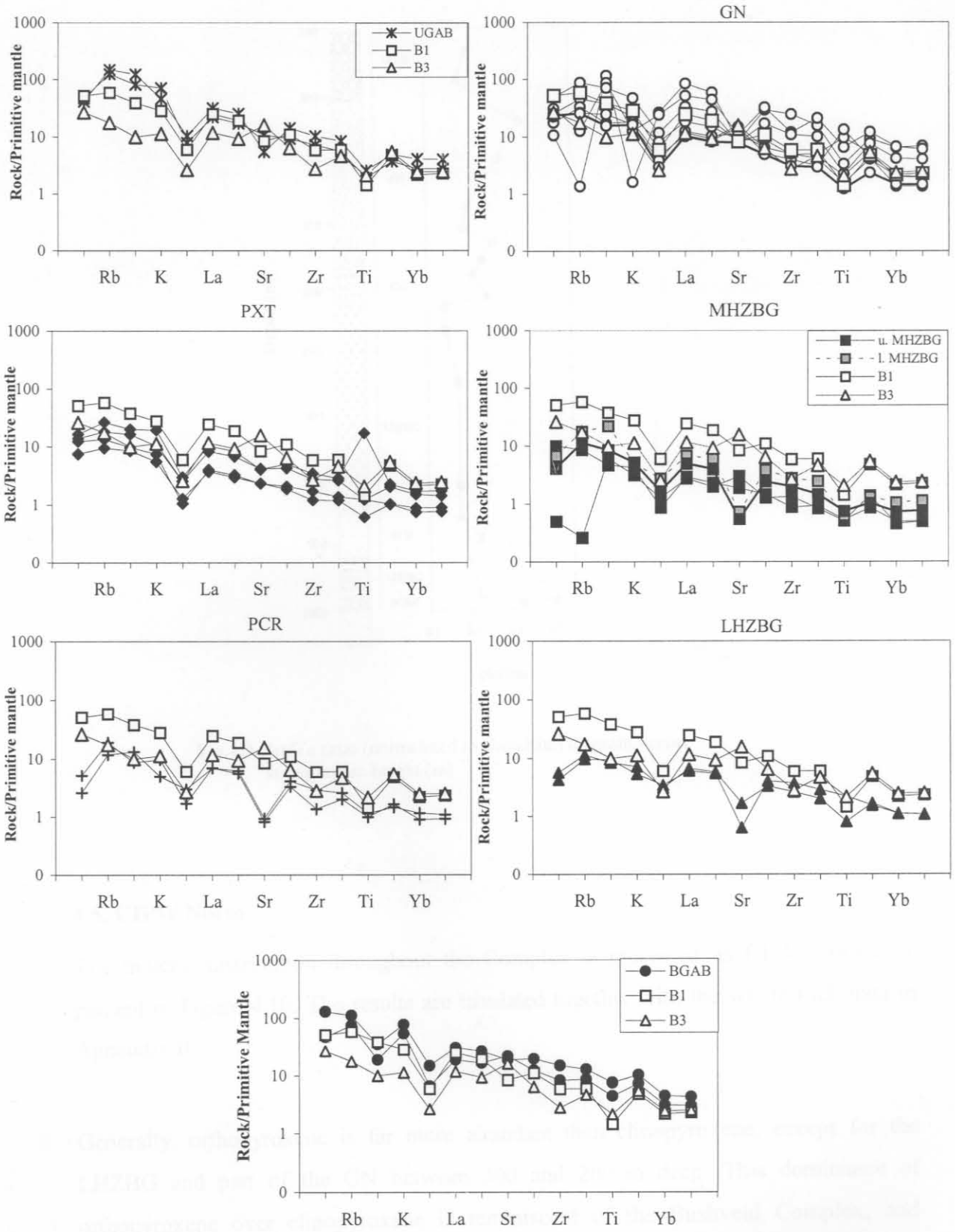

Fig. 4.8. Comparison between the average composition of B1-and B3-magmas and the different Units of the Utkomst Complex (B1 and B3 data from Curl, 2001. Mantle normalization factors are from Sun and McDonough, 1989).

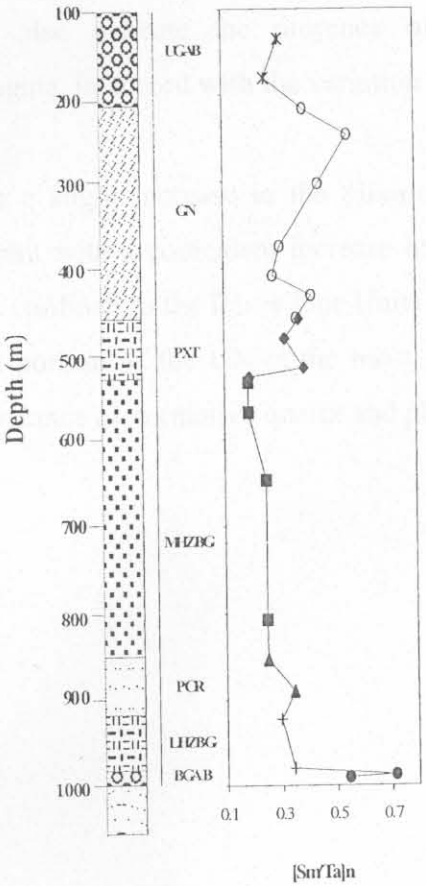

Fig.4.9. Sm/Ta ratio (normalized to chondrite) diagram versus stratigraphic height (m)

4.5. CIPW Norm

The mineral distribution throughout the Complex is presented as CIPW normative percent in Figure 4.10. The results are tabulated together with the whole rock data in Appendix II.

Generally, orthopyroxene is far more abundant than clinopyroxene, except for the LHZBG and part of the GN between 300 and 200 m deep. This dominance of orthopyroxene over clinopyroxene is reminiscent of the Bushveld Complex, and expected in view of the results of De Waal et al. (2001) who established a common age and magmatic lineage for the two complexes. The appearance of orthopyroxene before

clinopyroxene may also indicate the presence of a crustally derived siliceous component in the magma, in accord with the variation seen in Figure 4.9.

There appears to be a slight increase in the olivine content towards the top of the MHZBG, in agreement with a coincident increase in whole-rock Mg# (Fig. 4.6. (a)). Normative olivine is confined to the lower four Units and a few isolated samples in the GN. The uppermost portion of the GN is the most differentiated of the Complex as indicated by the abundance of normative quartz and plagioclase.

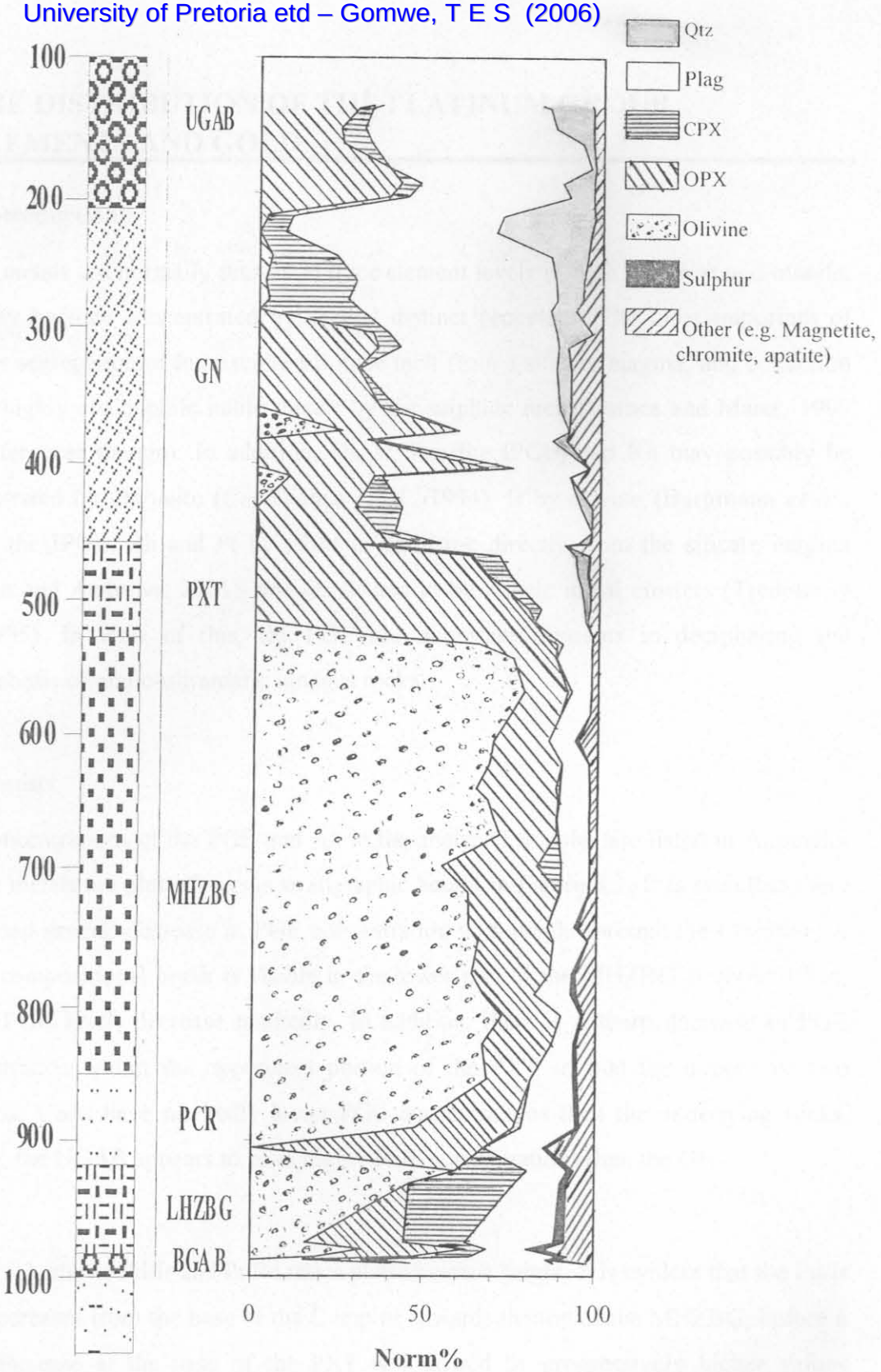

Fig. 4.10. Normalized data including sulphur concentrations Versus stratigraphic height (m)